Determination of NAD^+ and NADH level in a single cell under H_2O_2 stress by capillary electrophoresis

by

Wenjun Xie

A thesis submitted to the graduate faculty

in partial fulfillment of the requirements for the degree of

MASTER OF SCIENCE

Major: Analytical Chemistry

Program of Study Committee:
Edward S. Yeung, Major Professor
Robert S. Houk
Srdija Jeftinija

Iowa State University

Ames, Iowa

2008

To The Four Years

TABLE OF CONTENTS

LIST OF FIGURES

LIST OF TABLES

ABSTRACT

A capillary electrophoresis (CE) method is developed to determine both NAD^+ and NADH levels in a single cell, based on an enzymatic cycling reaction. The detection limit can reach down to 0.2 amol NAD^+ and 1 amol NADH on a home-made CE-LIF setup. The method showed good reproducibility and specificity. After an intact cell was injected into the inlet of a capillary and lysed using a Tesla coil, intracellular NAD^+ and NADH were separated, incubated with the cycling buffer, and quantified by the amount of fluorescent product generated. NADH and NAD^+ levels of single cells of three cell lines and primary astrocyte culture were determined using this method. Comparing cellular NAD^+ and NADH levels with and without exposure to oxidative stress induced by H_2O_2, it was found that H9c2 cells respond to the stress by reducing both cellular NAD^+ and NADH levels, while astrocytes respond by increasing cellular NADH/NAD^+ ratio.

CHAPTER 1. INTRODUCTION

NAD^+, NADH and their biological functions

β-Nicotinamide adenine dinucleotide, NAD^+, and its reduced form, NADH, are ubiquitous biomolecules found in both eukaryotic and prokaryotic organisms. Known as coenzymes, they transfer hydrogen atoms and electrons from one metabolite to another in many cellular redox reactions. During the process, it is the nicotinamide ring of the nucleotides that is oxidized or reduced (Figure 1). Particularly, NAD^+ and NADH are involved in cellular energy metabolism, including glycolysis, TCA cycle and oxidative phosphorylation, hence they are essential to the synthesis of ATP (Figure 2).

NADH is the substrate of over 300 cellular dehydrogenases, [1] including those located in the inner mitochondrial membrane and catalyzes the transfer of electrons from NADH to coenzyme Q during oxidative phosphorylation. Meanwhile, NAD^+ functions as a substrate for three other classes of enzymes in non-redox systems: 1) ADP-ribose transferases (ARTs) or poly(ADP-ribose) polymerases (PARPs), 2) cADP-ribose synthases and 3) sirtuins (histone deacetylases).[2] Interacting with these enzymes, NAD^+ and NADH play an important role in calcium homeostasis, DNA repair and gene expression.[3]

The NADH/NAD^+ ratio reflects the cellular metabolic status and redox state. It also regulates the cell redox state via enzymes such as the glycolytic dehydrogenases and the pyruvate dehydrogenase involved in acetyl-CoA synthesis in TCA cycle.[4] It has been reported that under oxidative stress, some cell types (erythrocyte, for example) increase their intracellular NADH/NAD^+ ratio or the NADH level in order to resist possible oxidative

damage.[3, 5, 6] Meanwhile, researchers of cell apoptotic mechanism argue that the exposure of cells to H_2O_2 leads to DNA single strand breakage and subsequently the activation of the DNA repair enzyme - PARPs. PARPs consume NAD^+ to form branched polyers of ADP-ribose on target proteins involved in DNA repair. The extensive activation of PARPs, however, may cause a critical reduction of cellular NAD^+ level and ultimately cell death (Figure 3).[7-10] In this case the determination of either NAD^+, or NADH, or NAD^+/NADH ratio is not adequate; only by monitoring both NAD^+ and NADH level change can we draw a real picture of how cells respond to oxidative stresses.

Intracellular NAD^+ and NADH levels are also related to cell proliferation,[11] sickle cell disease,[12] tumor development,[13] neoplasia and ischemia,[14] and a number of brain diseases.[2] Investigation of cellular NAD^+ and NADH levels and their variation in response to different environmental stimuli has been an important subject in the fields of biology, biochemistry and medicine. Pogue et al., for instance, have used NADH as a marker to assess cellular damage in tissues caused by photodynamic therapy (PDT), and found that the decrease in NADH was correlated to the PDT dose applied.[15]

Current approaches of NAD^+ and NADH analysis

The total concentration of NAD^+ and NADH in most cells is in the range of 10^{-3} M to 10^{-6} M. The ratio between the two varies from 1 to 700.[4] These nucleotides are found in cytosol, mitochondria, peroxisomes and other cellular compartments. Of all the intracellular NADH, only a portion is free; the rest is protein-bound.[16] Several methods are currently available for the determination of NAD^+ and NADH in cells and tissues. Most of these methods do not

differentiate NAD^+ and NADH location (in cytosol or in other compartments) or form (free or bound to proteins), but quantify the total amount of them.

Fluorescence microscope. NADH can be excited at 340nm and give off fluorescence at 460 nm, while NAD^+ is not fluorescent. The intrinsic fluorescence of NADH has enabled researchers to monitor NADH level in cells and tissues under fluorescence microscope. Karl et al. utilized two-photon NADH fluorescence to study the metabolic process in neurons and astrocytes during focal neural activity.[17] The imaging of NADH fluorescence is simple and has a high temporal resolution, but it is difficult to quantify NADH this way, and NAD^+ can not be directly monitored.

Enzymatic assays. To measure NADH in a biological sample, it is usually converted to NAD^+ (e.g., by using ethanol and alcohol dehydrogenase) and the decrease of fluorescence at 460 nm is related back to the original NADH concentration. Similarly, NAD^+ is measured by converting it to NADH and the increase of fluorescence is recorded.[18]

An enzymatic cycling assay for NAD^+ and NADH determination has been developed since 1960s, in which NAD^+ is reduced to NADH in one enzymatic reaction, and NADH is oxidized back to NAD^+ in another with the production of a colorimetric product.[19, 20, 21] Recently, a reaction with a fluorescent product was coupled into the enzymatic cycling system, making the method even more sensitive.[22, 23] By coupling the following two reactions:

$$NAD^+ + \text{lactate} \xrightarrow{\text{lactate dehydrogenase}} NADH + \text{pyruvate}$$

$$NADH + \text{resazurin} \xrightarrow{\text{diaphorase}} NAD^+ + \text{resorufin}$$

NAD^+ and NADH link an enzymatic reaction cycle:

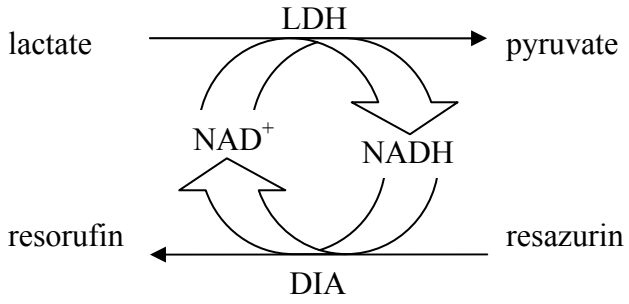

As the cycling goes on, a fluorescent product, resorufin, is formed, the accumulation rate of which is related to the amount of NAD^+ or NADH in the system. Since NAD^+ and NADH can both initiate the cycle, to quantify each of them in biological samples, the two nucleotides need to be extracted separately. NAD^+ is usually extracted in an acidic solution in which NADH is decomposed, while NADH is extracted in an alkaline solution in which NAD^+ is decomposed. Detection limit of NAD^+ as low as 0.2 nM (in a 200 μL reaction solution) using this method has been reported.[24]

Other methods. NAD^+ and NADH have also been quantified using HPLC and ESI-MS, yet detection limit of these methods are only at μM level with a bulk sample volume and pmol level, respectively.[25, 26] As NAD^+ and NADH in most cells falls on amol level, a more sensitive method is needed for single cell analysis.

Single cell capillary electrophoresis

Theoretically, any cellular component can be quantified as an average value based on a large population of identical cells. This approach works for homogenous cells cultured outside the body, but when it comes to a real tissue or organ such as the central nervous

system, there usually is big heterogeneity among the cells, biochemical processes of which are not always synchronized.[27] In such cases only single-cell study can reveal the variance among the cells and the kinetic changes across the tissue. Moreover, many diseases such as cancer start from only a few cells; with bulk analysis the signal from these abnormal cells are very likely to be masked by the large number of normal cells around, making it difficult to diagnose the diseases at an early stage.[28] The need to access information of individual cells has urged the research on single-cell analysis in recent years.

Capillary electrophoresis (CE) is among the early strategies used to determine different components inside single cells. The unique advantages of CE are 1) small sampling volume (comparable to that of a mammalian cell), 2) sensitive detection methods (such as laser-induced fluorescence, LIF) and 3) high separation efficiency. Single-cell CE is often carried out by injecting one cell into the capillary, breaking the cell membrane, separating the intracellular species and detecting the components of interest. Since the analytes can be separated from other intracellular species directly after a cell is drawn into the capillary and broken apart, this analytical method involves very little cell handling and no extraction procedure, thus introducing less disturbance to the cell content. Up to now, CE has been used to determine different classes of intracellular components in single cells, such as neurotransmitters, amino acids, enzymes and a number of metabolites.[27, 29-32]

CE-based enzymatic assay

Enzymatic reactions are often conducted in flow-control systems (chromatography, flow injection assay, capillary electrophoresis, etc.) in order to produce more reliable results than

off-line reactions. In these systems, efficient mixing of the reactants in a controllable manner is always an essential issue. For enzymatic assays carried out in a CE column, which is called electrophoretically mediated microanalysis or EMMA,[33] mixing is often based on the difference of migration rates of different reactants. With the continuous mode of EMMA, for example, the capillary is initially filled with running buffer containing one of the reactants while the other reactant is injected into the capillary as a sample plug. As separation voltage is applied and electrophoresis starts, the second reactant, which migrates either faster or slower than the first reactant in the running buffer, will catch up or be caught up by the first reactant. After the reactants are mixed, the flow is stopped to allow the reaction accumulate for a period of time. Then separation voltage is applied again and the products are driven to pass the detector. For enzymatic reactions with high turnover rate, the reaction may take place as soon as the reactants contact each other even before the incubating period, and continues as the reactants and products are driven through the capillary. This may lead to a frontal or tailing peak on the electropherogram.[34]

Overview of this work

In this study, a method of in-capillary enzymatic cycling assay is developed to determine NAD^+ and NADH content of a single cell. To show the applicable potential of this method in biological study, cells subjected to hydrogen peroxide are analyzed. Intracellular NAD^+ and NADH level change under these conditions provides information about how cells respond to oxidative stresses.

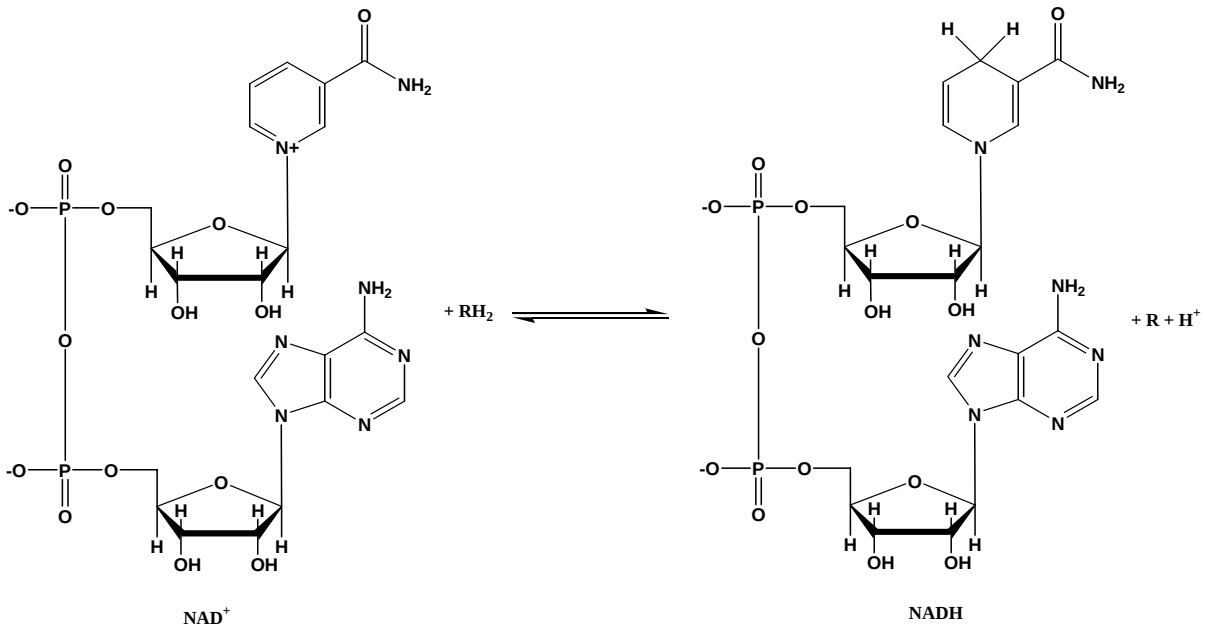

Figure 1. Chemical structures and conversion between NAD^+ and NADH.

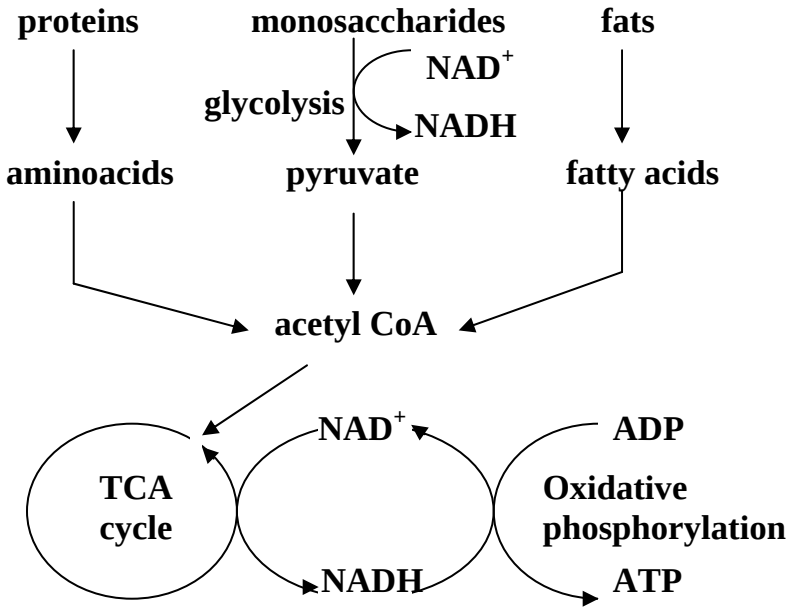

Figure 2. NAD^+ and NADH in cellular energy metabolism.

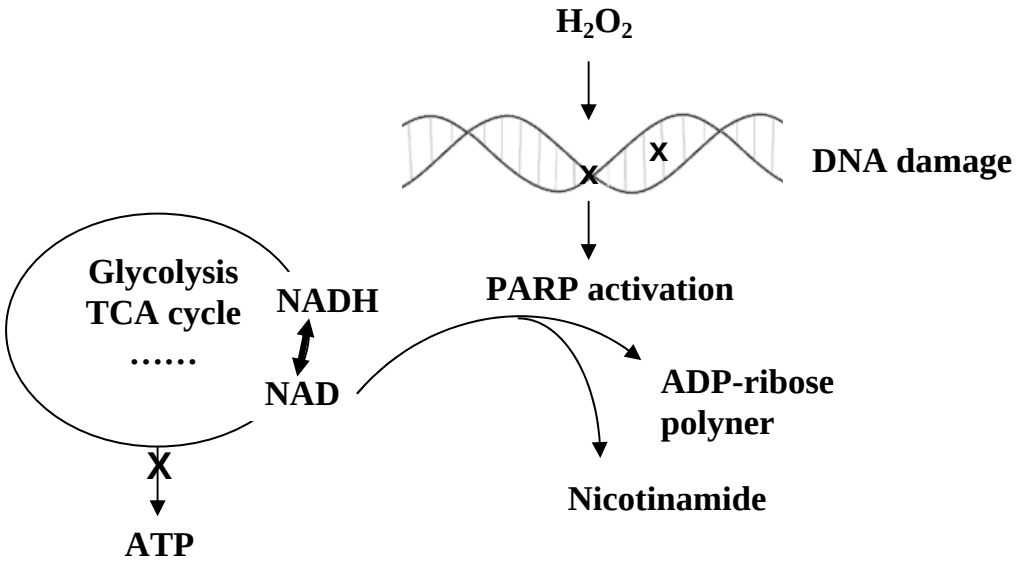

Figure 3. PARPs activation and NAD^+ depletion.

CHAPTER 2. EXPERIMENTAL SECTION

Reagents and chemicals

Lactate dehydrogenase (LDH, EC 1.1.1.27) was purchased from Calzyme Laboratories Inc (San Luis Obispo, CA, USA). Diaphorase (DIA, EC 1.6.99.-) was purchased from Shinko American Inc (New York, NY, USA). LDH and DIA were dialyzed against 20 mM sodium phosphate buffer for 24 hours before use. Resazurin was purchased from Invitrogen (Carlsbad, CA, USA) and dissolved in 50 mM pH 7.20 sodium phosphate buffer to make a 1 mM stock solution; this stock solution is extracted with chloroform at 4:6 (v/v) before use. Tris buffer (1.0 M pH 8.5) was purchased from Hampton Research (Aliso Viejo, CA, USA) and diluted to 100 mM without further adjustment. All other chemicals were purchased from Sigma-Aldrich (St. Louis, MO, USA) and used as received. Ultrapure water from a Mili-Q system (Milipore, Billerica, MA, USA) was used throughout the experiments.

Cell culture and cell treatment

Cell lines – NIH/3T3, a mouse fibroblast cell line, was cultured in Dulbecco's modified Eagle's medium (DMEM) supplemented with 10% bovine growth serum. MRC-5, a human lung fibroblast cell line, was cultured in EMEM supplemented with 10% fetal bovine serum. H9c2, a rat heart myoblast cell line, was cultured in DMEM supplemented with 10% fetal bovine serum. All three cell lines were purchased from American Type Culture Collection (Rockville, MD, USA). Cells were used between Passage 5 and Passage 12 starting from the purchased batch.

Astrocyte culture – Rat hippocampal and cortical astrocytes was obtained from Professor Srdija Jeftinija of Department of Biomedical Sciences, Iowa State University and cultured in DMEM supplemented with 10% fetal bovine serum. Cells were used no later than Passage 5.

For H_2O_2 treatment, cells in flask were placed in fresh medium and incubated with 100 μM H_2O_2 for 1 hour before they are harvested with trypsin. In PARPs inhibition study, 1 mM 3-aminobenzamide (3-AB) was added into the fresh medium 20 min before the addition of 100 μM H_2O_2. Cell number and viability were assessed by flow cytometry (EasyCD4 System, Guava Technologies, Hayward, CA, USA).

NAD^+ and NADH extraction

The harvested cells were rinsed with Hank's balanced salt solution (HBSS) twice and centrifuged down at 4.5×1000 rpm for 5 min. The cell pellet was resuspended in either 20% (v/v) trichloroacetic acid aqueous solution (to extract NAD^+) or 1 M potassium hydroxide solution (to extract NADH), placed on ice and processed by a probe sonicator for 1 min. The mixture was heated at 60 °C for 45 min and then centrifuged at 13×1000 rpm for 5 min. The supernatant was diluted in Tris buffer before analysis.

NAD^+ and NADH detection by capillary electrophoresis

NAD^+ and NADH were quantified separately on a single run using the enzymatic cycling assay coupled with capillary electrophoresis. As NAD^+ and NADH carry different charges, the two can be separated through capillary electrophoresis and the enzymatic cycling reaction takes place at the locations of NAD^+ and NADH in the capillary (Figure 4).

The full buffer here is used as both running buffer and reaction buffer, which is made of lactate, resazurin, LDH, DIA and Tris buffer (100 mM, pH 8.5). The capillary was first flushed and filled with the full buffer. After injection of samples (either a single cell or NAD(H) standards), electrophoresis was carried out for 3 min to separate NAD^+ and NADH. The electrophoretic flow was then stopped for 3 or 5 minutes. After that, separation voltage was turned on again until all the products were driven out. The baseline was allowed to return to the original level at the end of each run.

Instruments

A P/ACE™ capillary electrophoresis system (Beckman Coulter, Fullerton, CA, USA) was used with PDA detection mode and a 30 μm I.D., 365 μm O.D. fused silica capillary, 60 cm total length, 50 cm to detection window.

A home made capillary electrophoresis system was set up as previously described.[29, 30] Briefly, 22 kV was applied to a 20 μm I.D. and 365 μm O.D. fused silica capillary with a total length of 72 cm and 54 cm to detection window. The polyimide coating of a 5 mm section at the grounded end of the capillary was removed and the tip was etched with 40% hydrofluoric acid to about 60 μm O.D. This end of the capillary is used for injection and mounted on a 3-D translation stage to make it easy to switch between samples and running buffer. In the LIF detection system, a 543.5 nm, 5.0 mW He-Na laser (Melles Griot Corp., Irvine, CA, USA) was used as excitation source. A 1-cm focal length quartz lens was used to focus the laser to the optical detection window. Fluorescence from the window was collected by a photomultiplier tube (PMT, Model R928, Hamamatsu Corp, Bridgewater, NJ, USA)

through a 40× objective (Edmund Scientific Co., Barrington, NJ, USA) at a 90° angle to the laser beam. A 568 nm RazorEdge long-pass filter (Semrock, Rochester, NY, USA) was placed in front of the PMT. The other end of the capillary was inserted through a flexible septum into an airtight 20 mL glass buffer vial together with the high voltage electrode (Figure 5).

Cell injection. A chamber made by attaching a Teflon O-ring on a clean glass slide was used to hold cells or standard samples for injection (Figure 6). Cells suspended in HBSS were added into the chamber which was mounted close to the etched capillary tip, under the observation of a 60× bright field microscope. Single cells were injected via a pulse of vacuum exerted by pulling a 3 mL syringe inserted into the sealed buffer vial at the other end of the capillary. After an individual cell was drawn into the etched capillary tip, it was allowed to settle down to the capillary wall for 60s, during which the cell usually attaches to the capillary wall. A Tesla coil was then used to break the cell membrane (Figure 7).[30] A cell was usually lysed within 5 seconds this way, although no apparent morphological change can be observed. The capillary was then lifted up from the cell suspension and placed into a glass vial containing the running buffer. The entire process of cell injection takes about 2 minutes.

Injection of standard samples. NAD^+ and NADH standard samples (either alone or mixed) were made in 100 mM Tris buffer (pH 8.5) and added into the O-ring chamber. The samples were injected via electroosmotic flow by applying 22 kV for 3s. The injected volume was later calculated by relating to the migration rate of NAD^+ and NADH through the capillary under 22 kV, respectively. On each day of single cell analysis, the in-capillary enzymatic cycling assay was calibrated with NAD^+ and NADH standards.

Statistics

All results except those of single-cell analysis are represented as means ± standard error (SEM) on 3 observations. Student *t* test was used to compare data of two groups. *p* values less than 0.05 were considered statistically significant.

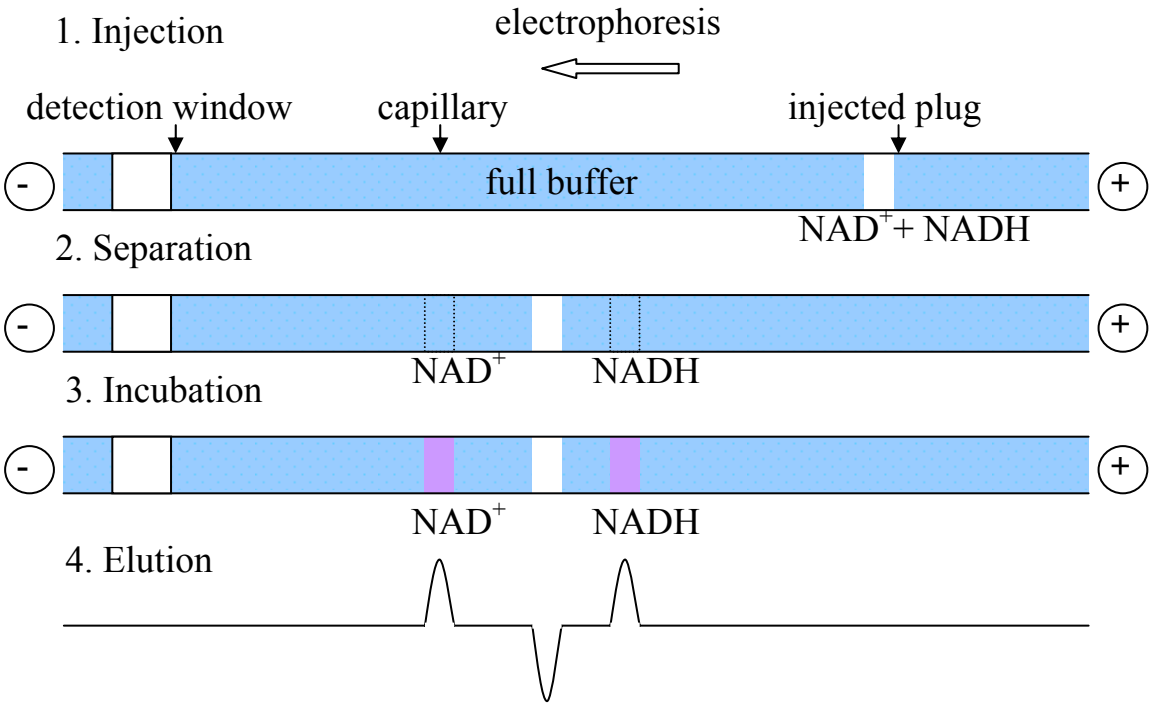

Figure 4. Scheme of the in-capillary enzymatic cycling assay for detecting of NAD^+ and NADH.

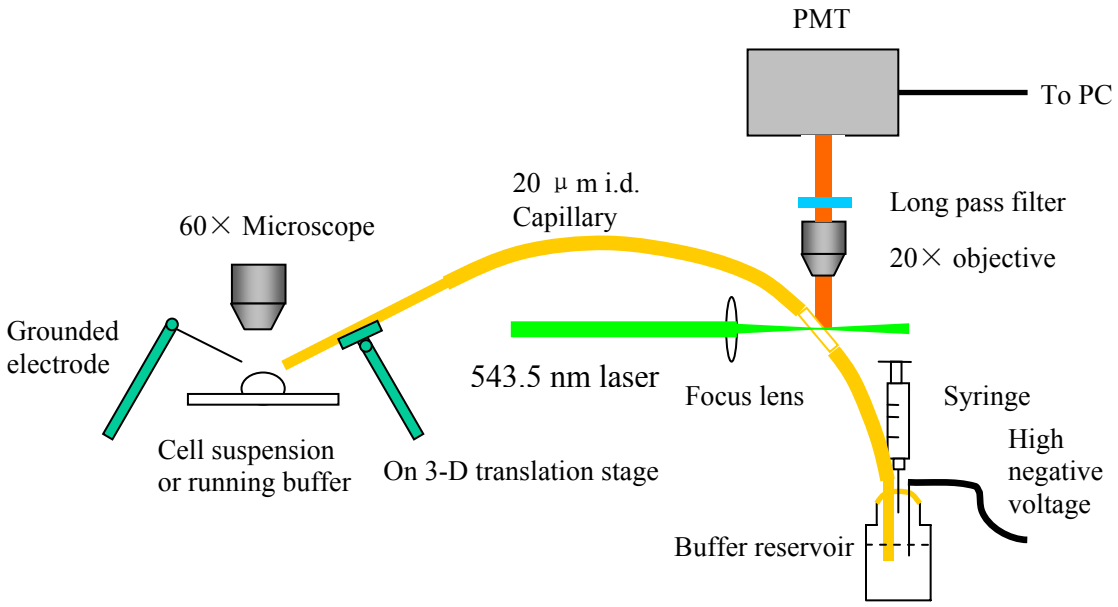

Figure 5. Configuration of the home-made capillary electrophoresis system.

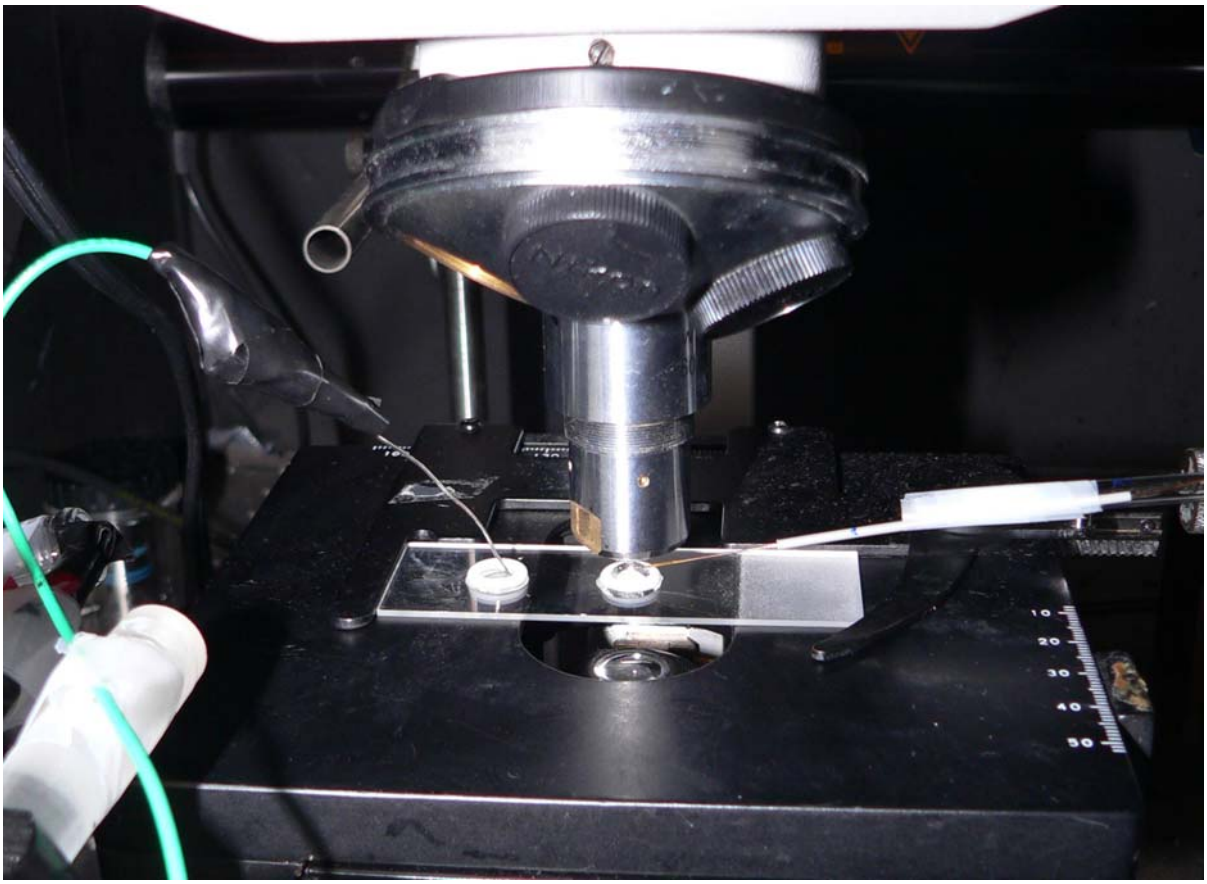

Figure 6. Photograph of the injection part of home-made capillary electrophoresis setup.

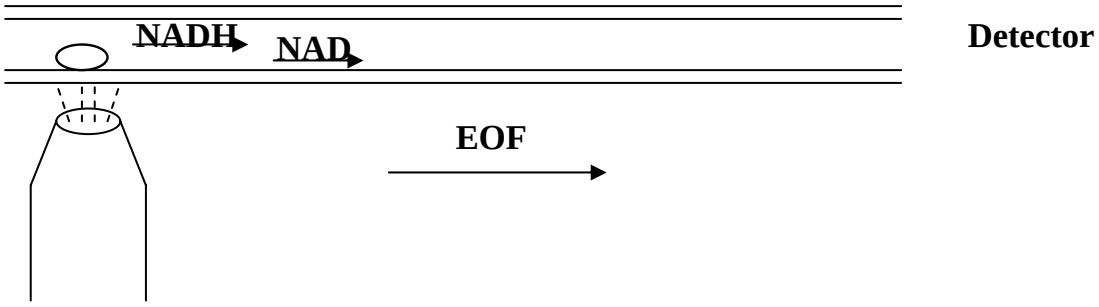

Figure 7. A cell injected into the capillary was lyzed using Tesla coil.

CHAPTER 3. RESULTS AND DISCUSSION

Enzymatic cycling assay in capillary

The enzymatic assay used in this study produces a fluorescent product, resorufin. This makes it possible to carry out the enzymatic cycling reaction in a capillary and detect the product with laser-induced-fluorescence (LIF) to achieve very low detection limit. Meanwhile, NAD^+ and NADH can be separated through capillary electrophoresis before they each induce the cycling reaction individually. Tested with buffers of different pH, it was found that the six components in the reaction can all be separated in 100 mM Tris buffer of pH 8.5 (Figure 8).

Among all the components in the cycle, NADH has the slowest migration rate while NAD^+ has the highest migration rate except lactate, which migrates much faster than the others. This means: 1) NAD^+ and NADH can be separated electrophoretically under this condition; 2) after being injected as a mixture, NAD^+ can catch up all the other reactants (except lactate which will catch up NAD^+) and NADH lags into all the other reactants, and the mixing will induce the cycling reaction.

Evaluation of the method

Detection limit and dynamic range of the online cycling method. Figure 9 shows that peaks corresponding to NAD^+ and NADH are separated after 3 minutes of electrophoresis and 3 minutes of incubation at room temperature. With longer incubation time and higher enzyme (both DIA and LDH) concentration, NAD^+ and NADH peaks are higher, and a better

detection limit can be achieved. The detection limit of this system is also dependent on the concentration of resazurin in the running buffer. As resazurin is weakly fluorescent at the detection wavelength (~ 580 nm), it causes a non-zero background to the running buffer, which rises as the concentration of resazurin goes up. Since the sample plug does not contain resazurin, it causes a negative peak when the adjacent NADH peak is not high and broad enough to cover it. A high background adversely affects the detection limit of the system, especially for NADH, the peak of which is immediately following the negative peak of the injected buffer plug. With a running buffer containing 0.2 U/mL LDH, 0.2 U/mL DIA, 0.5 mM lactate and 0.25 μM resazurin, the detection limit of NAD^+ can reach down to 0.2 nM, of NADH to 1 nM, which corresponds to 0.2 amol and 1 amol total amount. Yet limited by the low level of resazurin in the running buffer, the dynamic range of the system for detecting NAD^+ and NADH can not reach very high, only up to 200 nM for each. To determine the relatively high level of NAD^+ and NADH in mammalian cells, 1.5 μM resazurin is used in the running buffer, with which up to 1 μM NAD^+ and NADH can be quantified (Figure 10). The detection limits for both species, however, are compromised under this condition.

Reproducibility of the method. To assess the reproducibility of the in-capillary enzymatic cycling assay, 500 nM NAD^+ was run 6 times, with 0, 100, 200, 500, 800, 1000 nM NADH, respectively; the relative standard deviation (RSD) of the NAD^+-peak height is 0.040. Similarly, 500 nM NADH was also run 6 times with 0, 100, 200, 500, 800, 1000 nM NAD^+ and the RSD of the NADH-peak height is 0.050.

Specificity of the method. Five NAD(H) related compounds listed in Table 1, which are also present in cells, are tested using the same assay. 1 μM of each compound is analyzed; no significant interference with NAD^+ or NADH is found.

Reliability of single-cell assay. NAD^+ and NADH content of a single H9c2 cell under normal condition determined by the single-cell assay is in accordance with that obtained from cell extracts (Table 2). The results indicate that there is no significant error induced by the in-capillary cell lysing process. The cellular amount of NAD^+ and NADH determined here is also in the same range with reported data.[35]

Cell viability assessment

For cell lines, cell viability was higher than 90% under normal condition and there is no significant decrease (< 5%) under treatment with H_2O_2 or 3-aminobenzamide followed by H_2O_2.

Primary astrocyte culture has a lower viability even without treatment, around 80%. Exposure to H_2O_2 does not increase the death rate.

Single cell analysis

NIH/3T3 cells and MRC-5 cells. Single-cell electrophoregrams of the two cell lines are shown in Figure 11 and Figure 12. A single NIH/3T3 cell contains about 180×10^{-18} mole NAD^+ and 60×10^{-18} mole NADH. A single MRC-5 cell contains about 20×10^{-18} mole NAD^+ and 10×10^{-18} mole NADH. These data together with those from H9c2 cells are listed in

Table 3. There is a large variance in cellular NAD^+ and NADH level and NADH/NAD^+ ratio with different cell types.

H9c2 cells. The size of H9c2 cells varies from 10 μm to 40 μm in diameter, but most are around 20 μm, which were picked up for analysis. The electropherogram of NAD^+ and NADH from a single H9c2 cell is shown in Figure 13. NAD^+ and NADH content of 8 cells under normal condition, 6 cells treated with H_2O_2, and 7 cells treated with 3-aminobenzamide followed by H_2O_2 is shown in Figure 14. According to the results, each H9c2 cell under normal condition contains in average 780×10^{-18} mole NAD^+ and 110×10^{-18} mole NADH; NAD^+ level in cells exposed to 100 μM H_2O_2 for 1 hour decreased to 420×10^{-18} mole and NADH decreased to 40×10^{-18} mole; cells treated with 3-aminobenzamide and H_2O_2 remain NAD^+ level similar to that of normal cells ($P > 0.1$), with in average 670×10^{-18} mole NAD^+ and 4×10^{-18} mole NADH per cell. The NADH/NAD^+ ratio decreases from 0.15 under normal condition to 0.11 under H_2O_2, to 0.006 under H_2O_2 treatment with 3-aminobenzamide.

The trends of NAD^+ level change under H_2O_2 stress and with PARPs inhibitor are in agreement with Gilad et al.'s work,[36] in which the same cell line was treated with H_2O_2 to study myocardial oxidant injury. The results show that hydrogen peroxide causes DNA damage in H9c2 cells; PARPs are activated and consume intracellular NAD^+ to repair DNA; NADH is also reduced probably because part of it is converted to NAD^+. With the PARPs inhibitor 3-aminobenzamide around, hydrogen peroxide still induce DNA damage, but PARPs do not function to consume NAD^+; however, as the damage is not relieved, cells tend to die and intracellular NADH level, which is an indicator of cell viability, decreases, leading

to the decline of NADH/NAD^+ ratio. Whether a part of NAD^+ is converted to NADH is not known.

Primary astrocytes. The size of astrocytes varies more than that of the cell lines; accordingly, NAD^+ and NADH level in astrocytes varies significantly (Table 4). Unlike H9c2 cells, NADH/NAD^+ ratio in astrocytes increases under H_2O_2 treatment (Figure 15). This implies that astrocytes respond to H_2O_2 stress following a different mechanism than H9c2 cells. There has been no published work which deals with cellular NADH level change of astrocytes under H_2O_2 stress. There are similar studies done on yeasts, and the authors proposed that H_2O_2 might temporarily blocks the mitochondrial respiratory chain, so that NADH can not be oxidized to NAD^+, leading to temporal accumulation of NADH in the cell. Of course, different types of cells may respond to the same stimuli through totally different pathways. More investigations need to be done to verify whether the above presumption is true for astrocytes.

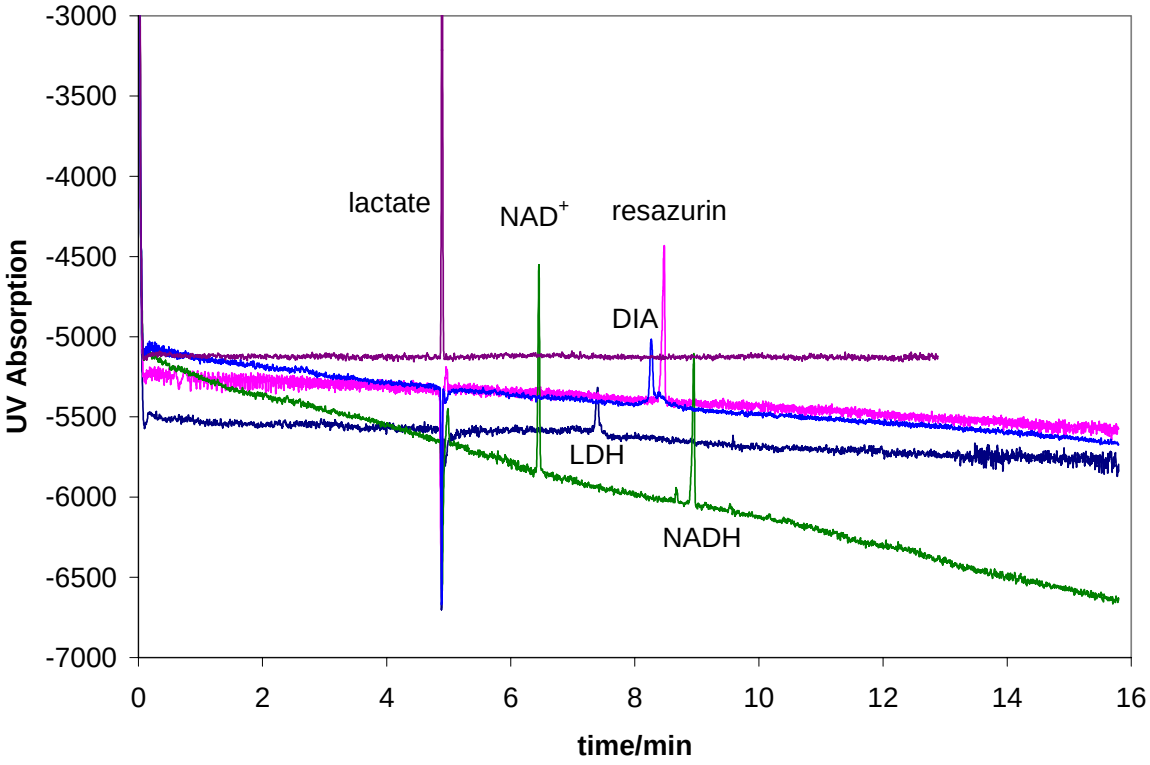

Figure 8. Electrophoregrams of the six components of the enzymatic cycling reaction in Tris buffer (100 mM, pH 8.5) on a Beckman P/ACE™ system.

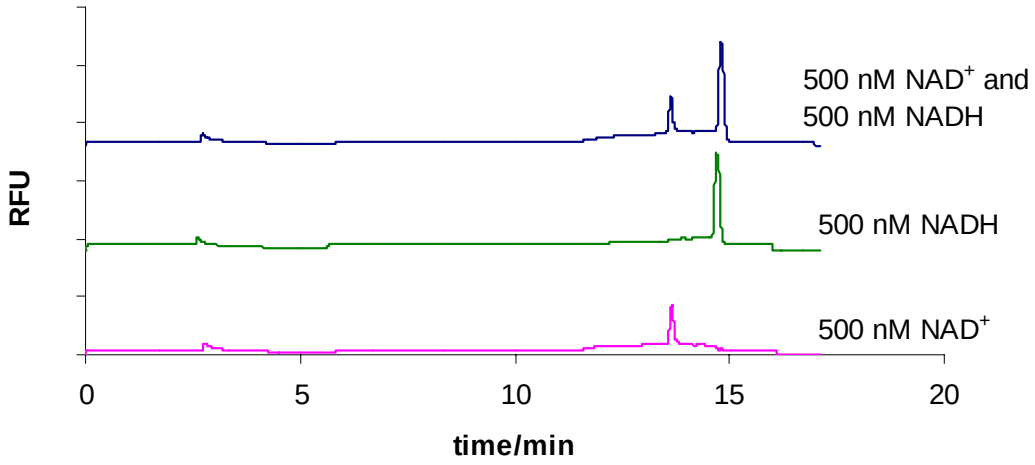

Figure 9. Separation and detection of 500 nM NAD^+ and 500 nM NADH.

The full running buffer used here containing 0.5 mM lactate, 1.5 uM resazurin, 0.1 U/mL LDH and 0.1 U/mL DIA, all in 100 mM Tris buffer (pH 8.5).

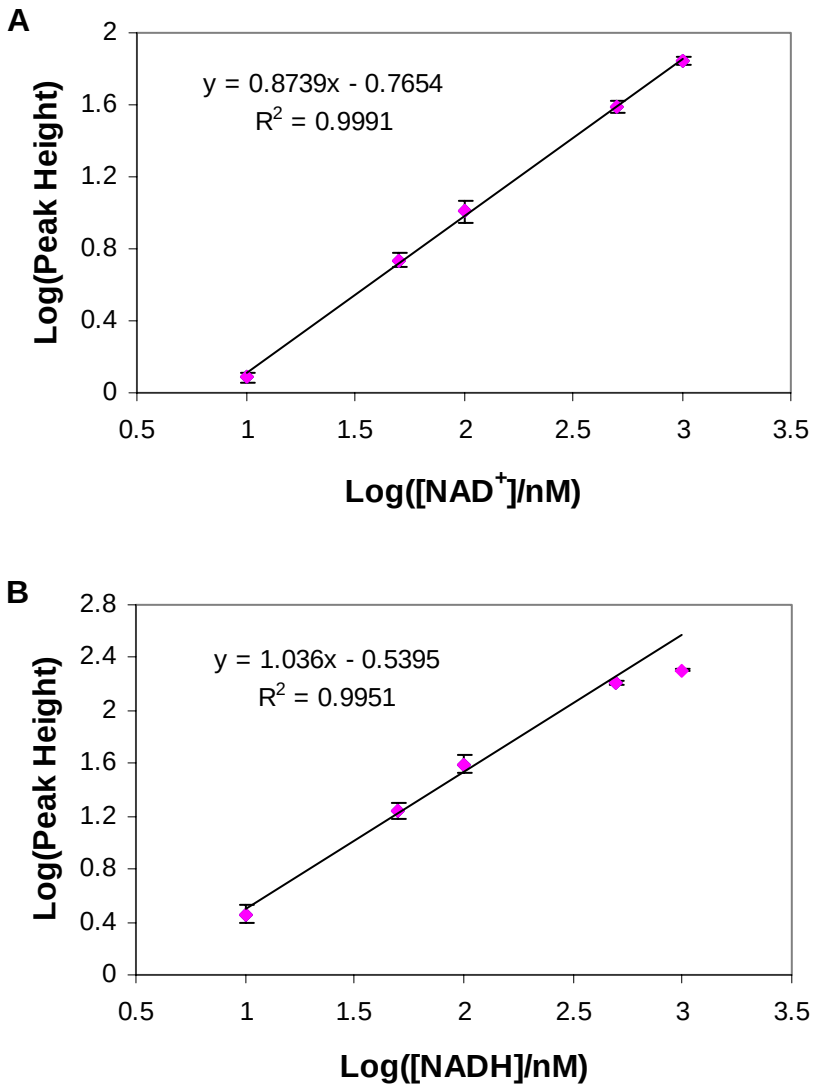

Figure 10. Fitting curves for NAD^+ detection (A) and NADH detection (B).

The full running buffer used here containing 0.5 mM lactate, 1.5 uM resazurin, 0.1 U/mL LDH and 0.1 U/mL DIA, all in 100 mM Tris buffer (pH 8.5).

Table 1. Interference study of NAD(H) related compounds.

Compound (1 μM)	Full name	Response as NAD^+	Response as NADH
NAD^+	nicotinamide adenine dinucleotide	100	---
NADH	reduced Nicotinamide adenine dinucleotide	---	100
$NADP^+$	nicotinamide adenine dinucleotide phosphate	0.2	0
NAAD	nicotinic acid adenine dinucleotide	0.3	0
NMN	nicotinamide mononucleotide	<0.1	0
NA	nicotinic acid	<0.1	0
NAM	nicotinamide	<0.1	0

Table 2. Amount of NAD^+ and NADH in a single H9c2 cell under normal condition.

NAD^+/amol		NADH/amol	
single cell analysis	cell extract analysis	single cell analysis	cell extract analysis
775 ± 84	726 ± 117	111 ± 60	108 ± 8

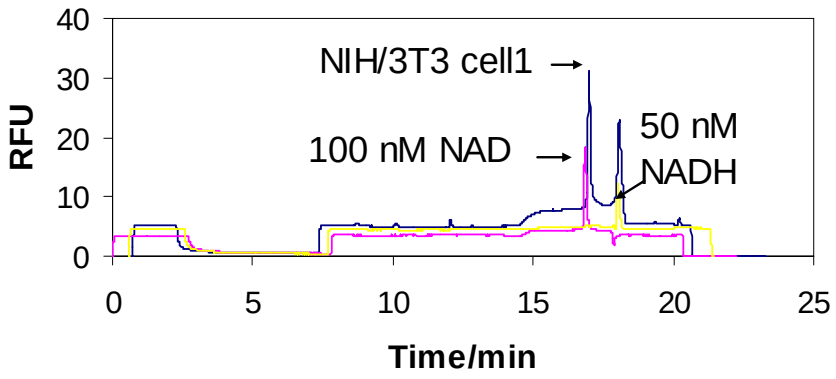

Figure 11. Identification of peaks of single NIH/3T3 cell analysis.

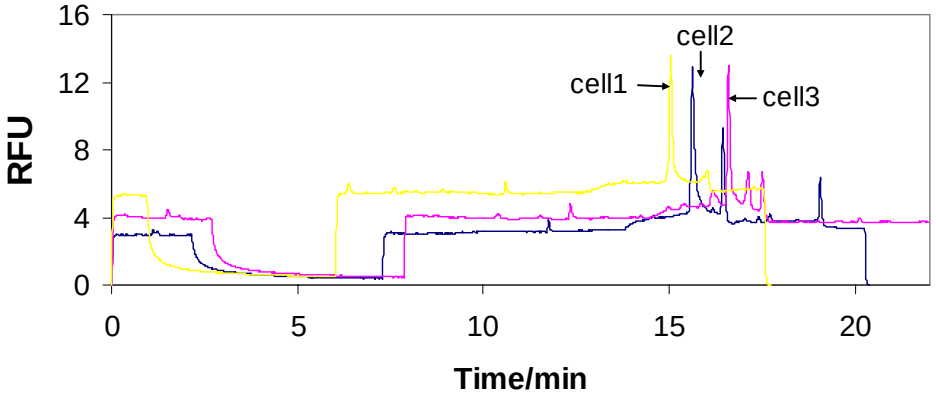

Figure 12. Electrophoregrams of single MRC-5 cell analysis.

Table 3. NAD^+ and NADH amount in single cells of different cell lines.

Cell type	NAD^+/amol	NADH/amol	$NADH/NAD^+$
NIH/3T3	180	60	0.33
MRC-5	20	10	0.50
H9c2	780	110	0.15

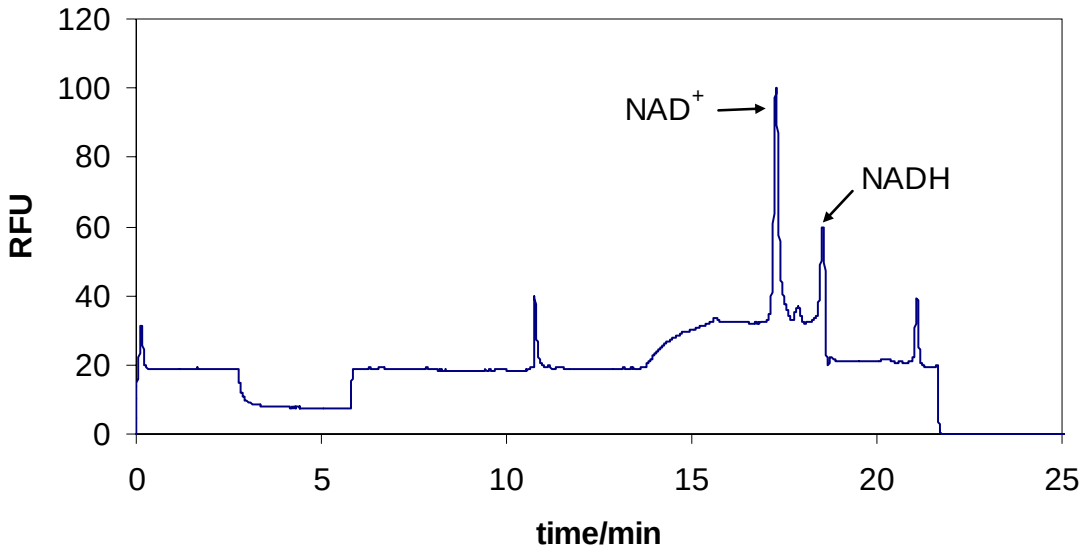

Figure 13. Electrophoregram of a single normal H9c2 cell analyzed by the enzymatic cycling assay.

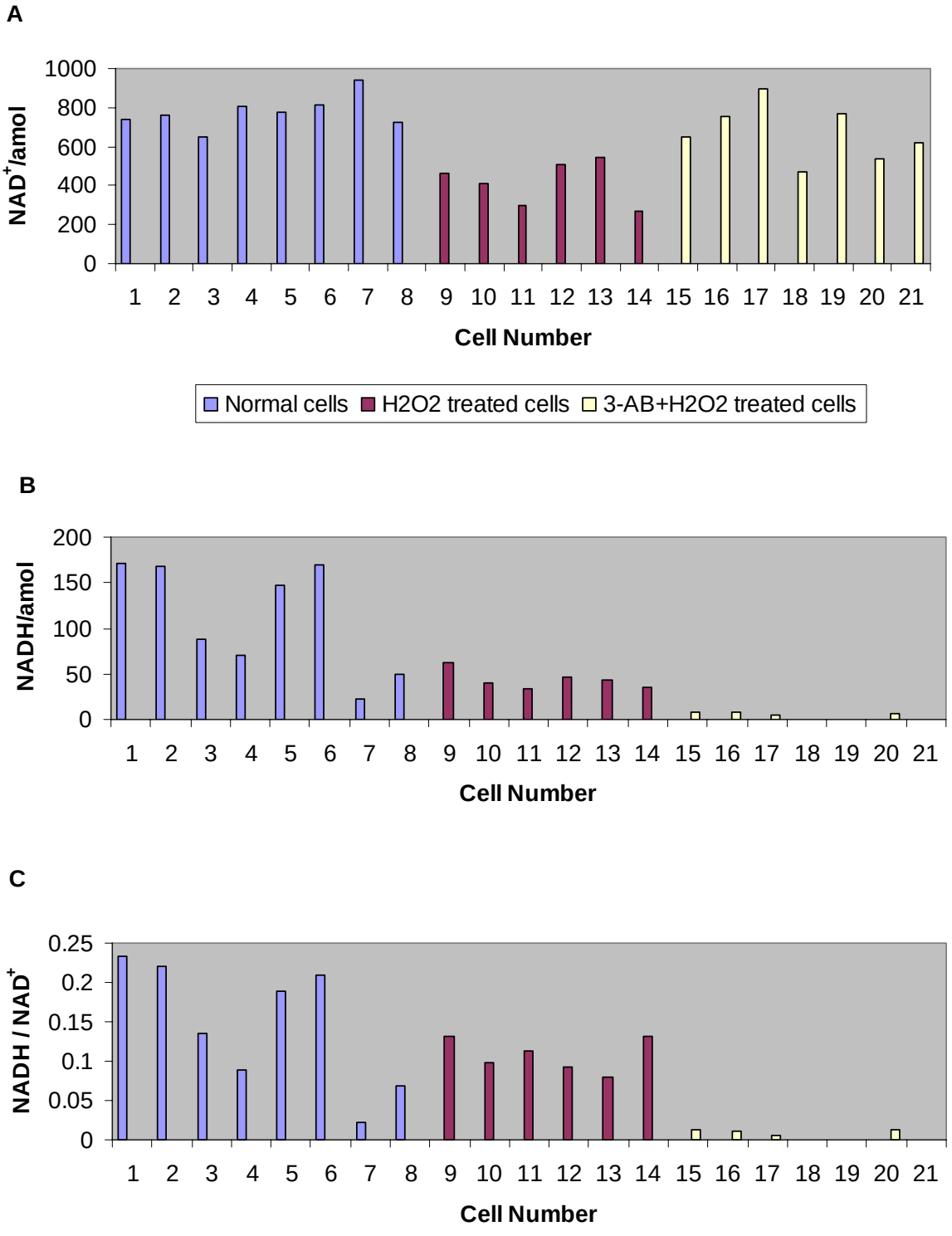

Figure 14. Single cell analysis results of (A) NAD^+; (B) NADH; (C) NADH/NAD^+ ratio of single H9c2 cells.

Table 4. NAD^+ and NADH amount in single astrocytes.

	under normal condition				under H_2O_2		
	NAD^+/amol	NADH/amol	NADH/NAD^+		NAD^+/amol	NADH/amol	NADH/NAD^+
Cell 1	266.08	69.66	0.2618	Cell 1	209.99	104.25	0.4965
Cell 2	180.78	60.11	0.3325	Cell 2	333.20	127.41	0.3824
Cell 3	248.78	49.78	0.2001	Cell 3	234.20	185.19	0.7908

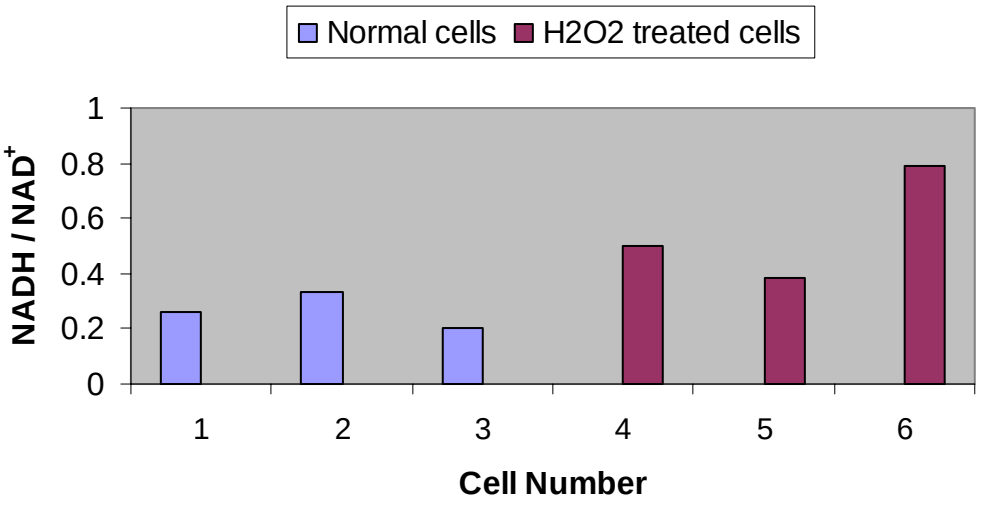

Figure 15. Cellular NADH/NAD^+ ratio of normal astrocytes and astrocytes treated with H_2O_2.

CHAPTER 4. CONLUSION

We have developed a new method to quantify coenzymes NAD^+ and NADH by coupling an enzymatic cycling reaction with capillary electrophoresis – LIF. This method is capable of separating and determining NAD^+ and NADH from a single cell in a single run. Detection limit of NAD^+ and NADH can reach down to 0.2 amol and 1 amol, respectively; the assay can measure NAD^+ and NADH up to 1 μM with higher concentration of resazurin in the reaction buffer. If other reactions can be incorporated into the same reaction buffer (e.g., converting $NADP^+$ to NADPH with glucose-6-phosphate and G6P dehydrogenase), other intracellular species such as $NADP^+$ and NADPH may also be separated and determined.

A parameter more interesting than the total amount of cellular NAD^+ and NADH is the amount of each nucleotide confined in different cell compartments such as in cytosol or mitochondria. Free NADH (in contrast with NADH bound to protein) has also been intriguing because it is directly correlated with many cellular reaction constants, but its quantification has been extremely difficult. If a gentler cell lysing process, which breaks down not the whole cell but only specific cellular compartments or does not disturb the binding of NADH to proteins, can be coupled with the CE-based assay in this work, compartmentalized NAD^+, NADH and free NADH would be determined.

Based on results of this study, 1 hour incubation with 100 μM H_2O_2 reduced both NAD^+ and NADH level in H9c2 cells. This change might be due to the activation of poly(ADP-ribose) polymerases in response to DNA damage, since the application of PARPs inhibitor, 3-aminobenzamide, prevents the reduction of NAD^+. It indicates that this dose of H_2O_2 and exposure time has been severe enough to cause DNA damage and cellular NAD^+ depletion;

NADH, which is in equilibrium with NAD^+, is reduced during the long incubation period correspondingly. The NADH/NAD^+ ratio declines significantly in cells treated with 3-aminobenzamide followed H_2O_2, though NAD^+ level is almost retained.

The same oxidative stress induces different response in primary astrocyte culture: the intracellular NADH/NAD^+ ratio increases to resist oxidative damage. Why different cells react to the same stimulus differently and the mechanism involved is a subject of interest.

REFERENCES

(1) Li, N.; Chen, G. *Talanta* **2002**, *57*, 961-967.

(2) Belenky, P.; Bogan, K. L.; Brenner C. *Trends in biochemical Sciences* **2007**, *32*, 12-19.

(3) Ying, W. *Frontiers in Bioscience* **2007**, *12*, 1863-1888.

(4) Lin, S. J.; Guarente, L. *Current Opinion in Cell Biology* **2003,** *15*, 241-246.

(5) Hwang, K.; Jeong, D. W.; Lee, J. W.; Kim, I. H.; Chang, H. I.; Kim, H. J.; Kim, I. Y. *Mol. Cells*. **1999**, *9*, 429-435.

(6) Liang, J.; Wu, W.; Liu, Z.; Mei, Y.; Cai, R. *Spectrochimica Acta Part A* **2007**, *67*, 355–359.

(7) Hudak, B. B.; Tufariello, J.; Sokolowski, J.; Maloney C.; Holm B. A. *AJP Lung Cellular and Molecular Physiology* **1995**, *269*, L59-L64.

(8) Gilad, E.; Zingarelli, B.; Salzman, A.L.; Szabo, C. *Journal of Molecular and Cellular Cardiology* **1997**, *29*, 2585-2597.

(9) Alano, C. C.; Ying, W.; Swanson, R. A. *Journal of Biological Chemistry* **2004**, *279*, 18895-18902.

(10) Szabo, C.; Dawson, V. L. *Trends in Pharmacological Sciences* **1998**. *19*, 287-298.

(11) Payot S.; Guedon E.; Gelhaye, E. *Research in Microbiology* **1999**, *150*, 465-473.

(12) Zerez, C. R.; Lachant, N. A.; Tanaka, K. R. *Blood* **1990**, *76*, 1008-1014.

(13) Zhang, Q. H.; Wang, S. Y.; Nottke, A. C. *Proc. Natl. Acad. Sci. U. S. A.* **2006**, *103*, 9029-9033.

(14) Lohmann, W.; Mussmann, J.; Lohmann, C. *Uropean Journal of Obstetrics Gynecology And Reproductive Biology* **1989**, *31*, 249-253.

(15) Pogue, B.W.; Pitts, J. D.; Mycek, M. A.; Sloboda, R. D.; Wilmot, C. M.; Brandsema, J. F.; O'Hara, J. A. *Photochemistry and Photobiology* **2001**, *74*, 817-824.

(16) Kasimova, M. R.; Grigiene, J.; Krab, K.; Hagedorn, P. H.; Flyvbjerg, H.; Andersen, P. E.; Moller, I. M. *Plant Cell* **2006**, *18*, 688-698.

(17) Kasischke, K. A.; Vishwasrao, H. D.; Fisher, P. J. *Science* **2004**, *305*, 99-103.

(18) Dekoning, W.; Vandam, K. *Analytical Biochemistry* **1992**, *204*, 118-123.

(19) Lowry, O. H.; Passonneau, J. V.; Schulz, D. W.; Rock, M. K. *The Journal of Biological Chemistry* **1961**, *236*, 2746-2755.

(20) Ying, W.; Garnier, P.; Swanson, R. A. *Biochemical and Biophysical Research Communications* **2003**, *308*, 809-813.

(21) Zerez, C. R.; Lee, S. J.; Tanaka, K. R. *Analytical Biochemistry* **1987**, *164*, 367-373.

(22) Bembenek, M. E.; Kuhn, E.; Mallender, W. D.; Pullen, L.; Li, P.; Parsons, T. *Assay and Drug Development Technologies* **2005**, *3*, 533-541.

(23) Graeff, R.; Lee, H. C. *Biochemical Journal* **2002**, *361*, 379-384.

(24) Cook, D. B.; Self, C. H. *Clinical Chemistry* **1993**, *39*, 965-971.

(25) Yamada, K.; Hara, N.; Shibata, T. *Analytical Biochemistry* **2006**, *352*, 282-285.

(26) Sadanaga-Akiyoshi, F.; Yao, H.; Tanuma, S. *Neurochemical Research* **2003**, *28*, 1227-1234.

(27) Wang, Z.; Yeung, E. S. *Journal of Chromatography B* **1997**, *695*, 59-65.

(28) Huang, W.; Ai, F.; Wang, Z.; Cheng, J. *Journal of Chromatography B* **2008**, *866*, 104-122.

(29) Hogan, B. L.; Yeung, E. S. *Analytical Chemistry* **1992**, *64*, 2841-2845.

(30) Xue, Q.; Yeung, E. S. *Journal of Chromatography B* **1996**, *677*, 233-240.

(31) Xue, Q.; Yeung, E. S. *Nature* **1995**, *373*, 681-683.

(32) Xue, Q.; Yeung, E. S. *Journal of Chromatography A* **1994**, *661*, 287-295.

(33) Zhang, J.; Hoogmartens, J.; Van Schepdael, A. *Electrophoresis* **2006**, 27, 35-43.

(34) Bao, J.; Regnier, F. E. *Journal of Chromatography* **1992**, *608*, 217-224.

(35) Hara, N.; Yamada, K.; Shibata, T. *Journal of Biological Chemistry* **2007**, *282*, 24574-24582.

(36) Gilad, E.; Zingarelli, B.; Salzman, A. L. *Journal of Molecular and Cellular Cardiology* **1997**. *29*, 2585-2597

AKNOWLEDGEMENT

I would like to express my sincere gratitude to my major advisor, Dr. Ed. Yeung, who has always been inspiring and supportive to his students. He set a real scientist model for me, which will encourage me to think deep and behave responsibly in my professional field.

I would also like to thank all the professors on my past and present POS committee, for their time and attention, especially Dr. Pat. Thiel and Dr. Robert Houk, who gave me huge positive confirmation; Dr. Rober Doyle and Dr. Srdija Jeftinija who helped me with cell cultures and taught me cell biology.

Thanks to all the members of the Yeung's group, Ji-Young Lee, Jiangwei Li, Aushuang Xu, Sangwon Cha, Hui Zhang, Ning Fang and others, who have taught and help me so much since I joined the group. Being alone in the United States, they are the first family I have here.

Finally, thank my parents for their endless love and support. Although they may never read about my work, the strength of their spirit is embedded deep in my every step.